Strategic and Probabilistic Aircraft Conflict Detection and Resolution for Three-Dimensional Trajectories

Eulalia Hernández-Romero*, Alfonso Valenzuela† and Damián Rivas‡
Department of Aerospace Engineering, Universidad de Sevilla
41092 Seville, Spain
Email:*ehernandez9, †avalenzuela, ‡drivas@us.es

***Abstract*—A probabilistic methodology for strategic aircraft conflict detection and resolution, up to 60 minutes in advance, under wind and temperature uncertainties is presented in this paper. The problem of hundreds of aircraft flying three-dimensional trajectories is considered. The conflict detection methodology is based on ensemble trajectory prediction, where the weather uncertainty data are retrieved from Ensemble Prediction Systems. The resolution trajectories are generated by modifying the trajectory waypoints (vectoring) with the aim of lowering the probabilities of the conflicts below a given safety threshold while maintaining low deviations from the nominal trajectories, using a metaheuristic approach. The methodology is applied to a realistic case study composed of actual flight plans in the European airspace.**

***Keywords*—Probabilistic conflict detection; probabilistic conflict resolution; weather uncertainty; Ensemble Prediction Systems.**

I. Introduction

The future of aviation presents many technical and operational challenges that demand an imminent modernization of the Air Traffic Management (ATM) system. Collaborative projects around the world, like the Single European Sky ATM Research (SESAR) and the Next Generation Air Transportation System (NextGen), work towards increasing the ATM system's capacity and efficiency, while maintaining, or even improving, its safety and sustainability. A promising approach towards meeting these goals is the development of automated decision support tools able to integrate and manage the uncertainty present in the ATM.

As discussed by Rivas and Vazquez [1], the ATM system is affected by several uncertainty sources, ranging from data uncertainty and unavailability to decisions taken by individuals. Among these sources, the effects of weather uncertainty on the ATM system are of utmost importance: the limited knowledge about present and future meteorological conditions is responsible for many delays and flight cancellations, negatively affecting ATM efficiency and translating into extra costs for aircraft operators.

In this paper, the problem of strategic aircraft conflict detection and resolution (CD&R) subject to weather uncertainty is analyzed. The large look-ahead horizon, up to one hour in advance, translates in high levels of uncertainty in the trajectory prediction. The proposed methodologies take into account and integrate wind and temperature uncertainty information available from probabilistic weather forecast into the conflict detection (CD) problem, allowing the computation of the pair-wise probabilities of conflict between the aircraft.

In this work, weather uncertainty data is retrieved from Ensemble Prediction Systems (EPS). This forecasting technique consists in running a deterministic Numerical Weather Prediction (NWP) model multiple times from slightly different initial conditions and/or with slightly perturbed weather models; some ensembles use more than one NWP model. Typically, an EPS is a collection of 10 to 50 forecasts, referred to as members; the uncertainty information is on the spread of the members. EPS are designed to sample the probability distribution function of the forecast and, frequently, the probability is estimated as a simple proportion of the ensemble members that predict an event to occur at a particular location or grid point [2]. The uncertainty information is on the spread of the members in the ensemble, and the hope is that this spread brackets the true weather outcome. The use of EPS in trajectory prediction and CD&R has been the subject of recent studies. Franco et al. [3] present a probabilistic trajectory predictor based on the Probabilistic Transformation Method (PTM) and apply it to the analysis of cruise flight time and fuel consumption considering wind uncertainties. Previous works by the authors [4], [5] also apply the PTM method to the CD&R problem for time horizons up to 20 minutes, a limited number of aircraft, and constant uncertain winds.

The methodology presented in this paper considers a time horizon of 60 minutes. It aims to expand the capabilities of conflict detection tools currently in use in Europe, such as Short-Term Conflict Alert (STCA) and Medium-Term Conflict Detection (MTCD), with time horizons of 2 and 20 minutes, respectively. Because the aircraft can travel hundreds of kilometers in one hour, the methodology is applied to a large airspace, as for example those handled by Area Control Centres, where hundreds of aircraft are simultaneously present.

Centralized conflict resolution (CR) is a highly combinatorial problem whose complexity significantly increases as the number of aircraft grows. Given the large number of aircraft considered in this work, a metaheuristic approach is convenient to tackle this problem. Metaheuristic techniques have already been used in large-scale CR problems by some authors,

including approaches based on genetic algorithm [6], memetic algorithm [7], or simulated annealing (SA) [8]. Following this last technique, Chaimatanan [9] uses a hybrid-metaheuristic approach based on SA to compute conflict-free trajectories on a continental scale; Courchelle et al. [10] also employ SA in strategic aircraft deconfliction covering a regional airspace. The CR methodology presented in this paper follows these last two works. An early version of this methodology, applied to two-dimensional trajectories, was presented in [11].

This study focuses on the CD&R problem of a large number of aircraft flying multi-segment three-dimensional trajectories subject to wind and temperature uncertainties. The wind and temperature data are retrieved from the European COSMO-D2-EPS. The CD methodology is based on ensemble trajectory prediction, where the aircraft trajectories are computed for each member of the ensemble to obtain an ensemble of trajectories; an efficient grid-based approach to conflict detection is used. The CR methodology uses the SA algorithm to generate resolution trajectories by modifying the coordinates of the trajectories' waypoints (vectoring). The objective is to lower the total probability of conflict between pairs of aircraft while minimizing the deviation from the nominal paths.

The paper is structured as follows. First, the problem formulation is presented in Section II, where the assumptions, equations of motion and the ensemble trajectory prediction approach are presented. Sections III and IV describe the conflict detection and conflict resolution methodologies, respectively. In Section V, a particular application considering air traffic in a wide area in central Europe and a given probabilistic weather forecast is described. Next, the results are presented in Section VI. Finally, the conclusions and future work are discussed in Section VII.

II. Problem Formulation

Let us consider N aircraft flying in the same airspace. Each aircraft $i \in [1, \ldots, N]$ follows a multi-segment 3D trajectory defined by K_i waypoints, whose positions (latitude, longitude and altitude) are provided by its flight plan. The aircraft horizontal trajectory is composed of straight segments and fly-by turns.

A. Assumptions

The following assumptions are taken into consideration:

- A spherical, non-rotating Earth model is considered, with radius R_E.
- A North-East reference system fixed to Earth is used (φ-axis pointing North and λ-axis pointing East). The vertical axis is pointing upwards, and the geometric altitude of the aircraft is assumed to be the same as the geopotential pressure altitude z_i.
- The aircraft motion is considered as that of a point mass with three degrees of freedom.
- The aircraft initial positions are certain and known.
- Each aircraft i flies with altitude-dependent Mach number, $M_i(z_i)$, or Calibrated Air Speed (CAS), $CAS_i(z_i)$, which are certain and known, as given by an operational procedure.
- The aircraft vertical speeds are given by their rate of climb or descent, $ROCD_i$. These values are dependent on the altitude, $ROCD_i = ROCD_i(z_i)$, and are also certain and known.
- The aircraft path angles are small, $\gamma_i \ll 1$.
- The aircraft are affected by horizontal uncertain winds, described by their zonal (West-East), w_λ, and meridional (South-North), w_φ, components. The air temperature, Θ, is also uncertain. The wind and temperature values for a particular location and time are provided by an Ensemble Prediction System.
- Turns are performed at constant radius. The turn radius of aircraft i, R_i, is that resulting from a constant bank angle, constant temperature given by the International Standard Atmosphere (ISA) at the altitude of each waypoint, and no winds.
- No turns are performed at the origin and destination waypoints of the trajectories.
- A quasi-steady state is assumed, thus the temporal and spatial derivatives of wind and temperature are negligible.

B. Equations of motion

By considering the previous assumptions, the equations that describe the movement of aircraft i can be expressed as the following system of differential equations:

$$\frac{d\varphi_i}{dt} = \frac{1}{R_E + z_i} V_{g,i} \cos\psi_i, \tag{1}$$

$$\cos\varphi_i \frac{d\lambda_i}{dt} = \frac{1}{R_E + z_i} V_{g,i} \sin\psi_i, \tag{2}$$

$$\frac{dz_i}{dt} = ROCD_i, \tag{3}$$

$$\frac{dr_i}{dt} = \frac{R_E}{R_E + z_i} V_{g,i}, \tag{4}$$

$$\frac{d\psi_i}{dt} = \frac{1}{R_i} \frac{dr_i}{dt}, \tag{5}$$

being λ_i and φ_i the aircraft longitude and latitude, ψ_i the aircraft course, r_i the ground distance along the trajectory, and $V_{g,i} = \|\vec{V}_{g,i}\|$ is the magnitude of the ground speed vector, which, because of the spatio-temporal dependence of the wind and the temperature, is different for each location and time, $\vec{V}_{g,i} = \vec{V}_{g,i}(\varphi_i, \lambda_i, z_i, t)$.

The straight segments of the trajectories are computed using Equations (1) to (4), with constant course, ψ_i. Turn segments are computed using Equations (1) to (5), considering constant turn radius, R_i.

The ground speed of aircraft i, assuming $\gamma_i \ll 1$, is computed from its airspeed V_i using the velocity triangle, depicted in Figure 1, as follows:

$$V_{g,i} = \sqrt{V_i^2 - w_{c,i}^2} + w_{a,i}. \tag{6}$$

In this equation, $w_{c,i}$ and $w_{a,i}$ are the cross-track and along-track components of the wind affecting the aircraft, respectively, which can be obtained from the zonal and meridional

wind components given by the weather forecast, for each location and time ($w_\lambda(\varphi_i, \lambda_i, z_i, t)$ and $w_\varphi(\varphi_i, \lambda_i, z_i, t)$):

$$w_{c,i} = w_\lambda \cos\psi_i - w_\varphi \sin\psi_i, \tag{7}$$

$$w_{a,i} = w_\lambda \sin\psi_i + w_\varphi \cos\psi_i. \tag{8}$$

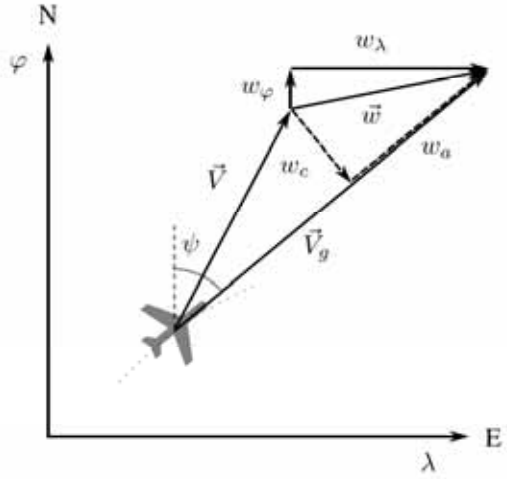

Figure 1. Velocity triangle for aircraft i.

The aircraft airspeed, V_i, can be computed from its Mach number, M_i, or Calibrated Air Speed, CAS_i, as defined by an operational procedure. The functions that describe these relations are dependent on the atmospheric temperature, which is obtained from each ensemble member and varies with time and location, $\Theta = \Theta(\varphi_i, \lambda_i, z_i, t)$.

In this paper, the wind and temperature values for a particular location and time are linearly interpolated from the gridded data provided by the EPS. Because the wind components and the air temperature are uncertain, the aircraft ground speeds are also uncertain, and so are their positions along the trajectory at a given time. In this paper, ensemble trajectory prediction is used to compute the possible future states of the aircraft: the differential equations previously presented are integrated for each one of the M members of the EPS, resulting in an ensemble of M different trajectories for each aircraft which captures the uncertainty in the prediction.

III. Conflict Detection

A conflict between two aircraft exists when their future positions are predicted to be closer than a given set of separation minima (i.e. a horizontal distance D and a vertical distance H). In order to analytically determine the existence of a conflict, the normalized distance of closest approach between aircraft i and j, δ_{ij}, is defined as

$$\delta_{ij} = \min_t \left(\max \left\{ \frac{d_{ij}(t)}{D}, \frac{h_{ij}(t)}{H} \right\} \right), \tag{9}$$

where $d_{ij}(t)$ and $h_{ij}(t)$ are the horizontal and vertical separations between aircraft i and j at time t, respectively. The aircraft i and j are considered to be in conflict if the following condition holds:

$$\delta_{ij} < 1. \tag{10}$$

An ensemble approach to conflict detection is used in this work. The procedure to obtain the probability of conflict between aircraft i and j is the following:

1) For each member of the ensemble, $m \in [1, \ldots, M]$, the distance of closest approach between i and j, $\delta_{ij,m}$, is determined.
2) A conflict in member m between i and j, $c_{ij,m}$, is identified if $\delta_{ij,m}$ is less than the minimum separation requirement:

$$c_{ij,m} = \begin{cases} 1 & \text{if } \delta_{ij,m} < 1, \\ 0 & \text{if } \delta_{ij,m} \geq 1. \end{cases} \tag{11}$$

3) Considering that all the members are equally probable, the probability of conflict between i and j, $P_{con,ij}$, is computed as the fraction of members for which a conflict is identified:

$$P_{con,ij} = \frac{1}{M} \sum_{m=1}^{M} c_{ij,m}. \tag{12}$$

The probability of conflict is pairwise determined for the N aircraft. In order to alleviate the computational effort of determining the minimum distance for all the aircraft pairs, a grid-based conflict detection scheme is used. Using this procedure, each trajectory is discretized and stored into the cells of a grid; then, the conflict between two aircraft is computed only if the cells assigned to their trajectories are either coincident or adjacent [12].

The application of this method to the proposed probabilistic CD is as follows. For each one of the M members of the ensemble, a four-dimensional grid (longitude, latitude, altitude, and time) is constructed, as illustrated in Figure 2. In each cell of the grid, a list of the aircraft occupying the cell is stored. The minimum distance between aircraft i and j, $\delta_{ij,m}$, is computed only if their trajectories occupy coincident or adjacent cells, and the conflict is characterized using Equation (11); otherwise, $\delta_{ij,m}$ is not computed and the variable $c_{ij,m}$ is directly set to zero. This method is suitable for parallelization; the conflict detection for each ensemble member and aircraft pair can be performed independently.

IV. Conflict Resolution

In this work, vectoring is chosen as the resolution maneuver, that is, conflicts are solved by modifying the coordinates of the trajectories' waypoints. Only the horizontal position of the waypoints is modified. The conflict resolution problem is formulated as an optimization problem, which is solved using the Simulated Annealing algorithm.

A. Decision variables

The decision variables in the optimization problem, $\mathbf{u} = \{\mathbf{u}_1, \mathbf{u}_2, \ldots, \mathbf{u}_i, \ldots, \mathbf{u}_N\}, i = 1, \ldots, N$, are the coordinates of the modifiable waypoints of each aircraft trajectory; all the waypoints that define the flight path, with the exception of the initial and final points of the trajectory, are considered as modifiable.

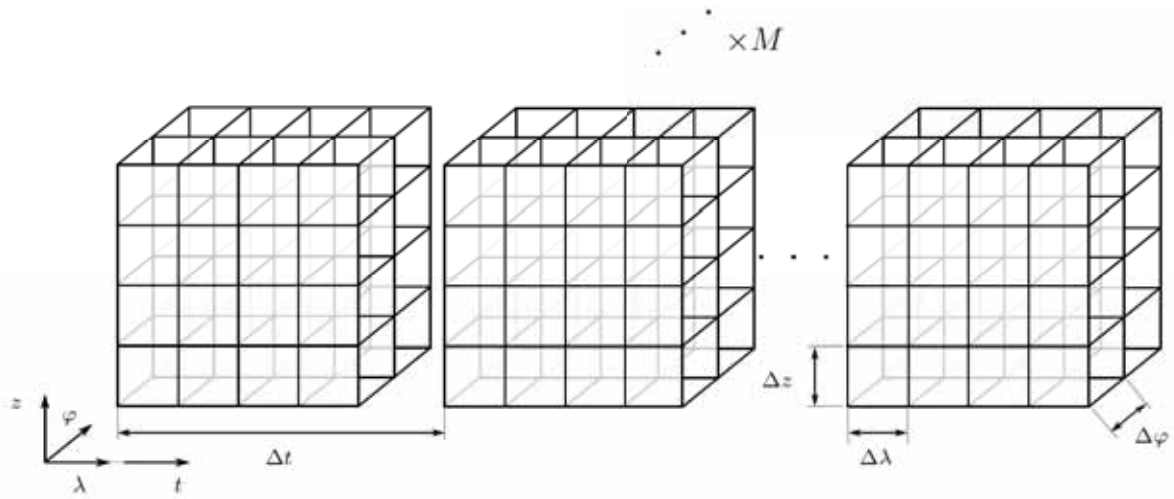

Figure 2. Four-dimensional (3D space and time) grids.

For aircraft i, the decision variables are collected in a control matrix $\mathbf{u}_i$. Each row of this matrix, $\mathbf{u}_{ik}$, corresponds to one modifiable waypoint. The first element is the longitude of the waypoint, and the second element is its latitude:

$$\mathbf{u}_{ik} = [u_{ik_\lambda}, u_{ik_\varphi}], \qquad k = 1, \ldots, K_i - 2. \tag{13}$$

In this expression, K_i is the total number of waypoints in the trajectory of aircraft i, as given by its flight plan. An example is illustrated in Figure 3. In this figure, the nominal path of the aircraft, collected in the matrix $\mathbf{u}_i^0$, is also depicted. The total number of modifiable parameters is $q = 2\sum_{i=1}^{N}(K_i - 2)$.

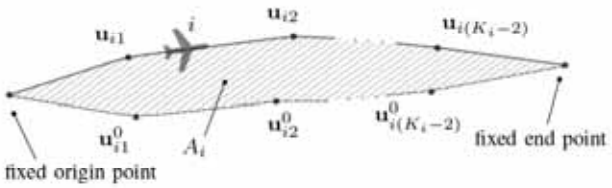

Figure 3. Decision variables for aircraft i.

B. Constraints

The decision variables are subject to two kinds of constraints:

1) The distance between consecutive waypoints k and $k+1$, $\|\mathbf{u}_{ik} - \mathbf{u}_{ik+1}\|$, must be large enough to accommodate the fly-by turns performed at the each waypoint. This constrain can be expressed as:

$$\|\mathbf{u}_{ik} - \mathbf{u}_{ik+1}\| \geq L_{ik} + L_{ik+1}, \tag{14}$$

$$L_{ik} = R_i \tan(\alpha_{ik}/2), \tag{15}$$

where L_{ik} is the distance between waypoint k and the start/ending point of the turn, and α_{ik} is the course change at waypoint k. Since no turns are performed at the origin and destination waypoints, L_{i1} and L_{iK_i} are nil.

2) To prevent large lateral deviations, the possible locations of the modified waypoints $\mathbf{u}_{ik}$ are bounded:

$$u_{ik_\lambda} \in [u^0_{ik_\lambda} - \delta\lambda/2, u^0_{ik_\lambda} + \delta\lambda/2], \tag{16}$$

$$u_{ik_\varphi} \in [u^0_{ik_\varphi} - \delta\varphi/2, u^0_{ik_\varphi} + \delta\varphi/2], \tag{17}$$

where $\delta\lambda$ and $\delta\varphi$ are configurable limits.

C. Cost function

The objective of the conflict resolution is to minimize the probabilities of conflict between pairs of aircraft while minimizing the deviation from the nominal paths. Taking this into account, the following cost function J is used:

$$J = \sum_{i=1}^{N} J_i = \sum_{i=1}^{N} \left(\frac{1}{2} \sum_{j=1, j\neq i}^{N} (C_{ij} - \eta_{ij}) + \zeta \frac{A_i}{L_{0,i}} \right). \tag{18}$$

where J_i is the cost related to trajectory i.

The variable C_{ij} represents the conflict probability between aircraft i and j; it is defined as:

$$C_{ij} = \begin{cases} P_{con,ij} & \text{if } P_{con,ij} \geq P_\tau \\ 0 & \text{if } P_{con,ij} < P_\tau \end{cases}, \tag{19}$$

where P_τ is the considered probability threshold. This threshold aims at differentiating between low- and high-probability conflicts (below and above the threshold, respectively). The objective is to focus the resolution effort on more demanding conflicts and avoid wasting resources on conflicts which may not materialize.

Since the presented methodology is envisioned for strategic resolution, those aircraft that are in loss of separation at the time of the prediction should be solved by tactical tools, and are disregarded from this process. The variable η_{ij} addresses this idea by removing the cost of these losses of separation from the cost function. This variable takes value one if aircraft i and j are in loss of separation at their initial positions and zero otherwise; note that, when a tactical conflict between i and j takes place, the variable C_{ij} also takes value one. Finally, A_i is the area between the modified and the nominal path of

aircraft i (defined by $\mathbf{u}_i$ and $\mathbf{u}_i^0$), as depicted in Figure 3, and $L_{0,i}$ is the total flight distance of the nominal trajectory. The ratio $A_i/L_{0,i}$ is an evaluation of the lateral deviation from the original intent. The coefficient ζ is a configurable weight parameter used to balance the resolution of conflicts and the deviations from the nominal paths; this coefficient should be small enough so that this last term does not overpower the other.

D. Simulated Annealing

In this work, hundreds of aircraft are simultaneously handled, deriving into thousands of decisions variables. Due to this complexity, a metaheuristic approach is employed. The simulated annealing algorithm is chosen to solve the optimization problem. Simulated annealing is a technique introduced in 1983 by Kirkpatrick et al. [13], inspired by the annealing process in metallurgy.

The basics of the SA algorithm applied to the proposed CR methodology are as follows. A temperature T is used as a control parameter. For a given temperature, an iterative process is conducted: at each iteration, the aircraft trajectories are modified according to a neighborhood function; on the one hand, if the new trajectories improve the value of the current cost function, the modification will be accepted; on the other hand, if the modification does not improve the objective function value, it will only be accepted with a certain probability of acceptance that decreases as the temperature decreases. The neighborhood function used in the algorithm prioritizes changes in the aircraft trajectories that contribute the most to the value of the cost function, while also guaranteeing that the problem constraints detailed in Section IV-B are met. When a predefined number of iterations is reached, then the temperature is decreased according to a chosen cooling schedule. The process is then repeated until a target value of T is reached, so as the probability of acceptance is sufficiently small. A detailed description of the proposed algorithm can be found in [11].

V. Application

In this section, the case study used to illustrate the application of the proposed methodology is presented. The CD&R process is launched at a given day at 12:00 UTC, and conflicts are detected and solved for the next 60 minutes.

The weather uncertainty is retrieved from the ensemble prediction system COSMO-D2-EPS, developed and operated by the German Weather Service [14], [15]. This EPS is a 20-member ensemble which covers a wide area in central Europe (see Figure 4). The forecast is operated for the very short-range, has a fine-scale horizontal resolution of 2.2 km, and vertical resolution of 65 atmosphere levels. It is run at 00, 03, 06, 09, 12, 15, 18 and 21 UTC, providing hourly forecasts up to 27 hours. They are available about one hour after the run. In particular, the forecast for the 26th of September of 2019, run at 09:00 UTC with lead times of 3 and 4 hours, is used. The products used in this application are the meridional and zonal wind components, and the temperature for nine different pressure levels: 200, 300, 400, 500, 700, 850, 950, 975, and 1000 hPa. For example, Figure 4 represents the mean value for the zonal wind component corresponding to pressure level 200 hPa. The figure also illustrates the coverage area of the forecast.

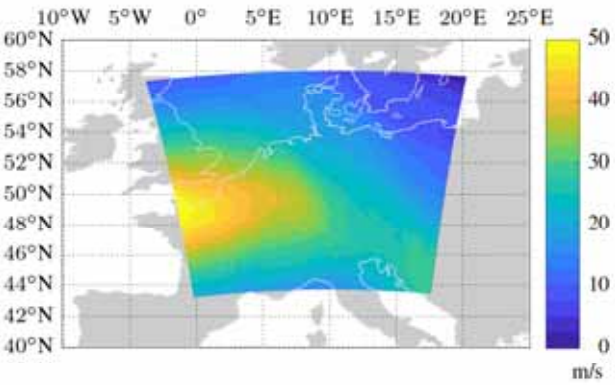

Figure 4. COSMO-D2-EPS: average zonal wind at pressure level 200 hPa. 3-hour forecast ran at 9:00 UTC 2019-09-26.

The air traffic over Europe the 14th of February of 2019 inside the EPS coverage area is considered. The flight data are collected from the last filed flight plans stored in Eurocontrol's Demand Data Repository [1] (DDR). The aircraft speeds (Mach number, calibrated airspeed CAS and rate of climb or descent ROCD) and bank angle values are obtained from Eurocontrol's Base of Aircraft Data (BADA 3.13) [16], which establishes the following operational procedures: CAS-Mach climbs (changing at a transition altitude), constant Mach cruises, and Mach-CAS descents (changing at a transition altitude). Flights inside the EPS coverage area that fly above 10000 ft (flight level FL100) at 12:00 are considered, resulting in a scenario with $N = 822$ aircraft. Those aircraft that at the starting time are not above FL100 nor in the designated area are not considered. The total number of free variables in the optimization problem for this traffic scenario is $q = 11156$.

VI. Results

The results presented in this section aim at illustrating the capabilities of the proposed methodology, describing and analyzing the CD&R outcome for the aforementioned application.

The separation requirements are $D = 5$ NM and $H = 1000$ ft. The 4D grid used in the conflict detection phase has a size of $\Delta\lambda = \Delta\varphi = 0.1°$, $\Delta h = 1000$ ft$= 304.8$ m, and $\Delta t = 1$ s. The probability of conflict threshold is $P_\tau = 50\%$, and the cost-function weight coefficient is set to $\zeta = 0.1$ m^{-1}. The rest of the parameters used in the conflict resolution process are: $I = 200$, $\tau_0 = 40\%$, $\beta_{SA} = 0.98$, $\gamma_{SA} = 10^{-3}$, and $\delta\lambda = \delta\varphi = 0.3°$ (see [11]).

As an example of the effects of the methodology on the aircraft trajectories, Figure 5(a) shows the normalized distance (δ_{AB}) between two aircraft A and B over time, for each member of the ensemble, before and after the conflict resolution. The dash-dotted line at 1 represents the minimum separation

[1] https://www.eurocontrol.int/ddr

requirement. Before the CR process, a conflict is detected for all members of the ensemble at around 16 minutes, leading to a probability of conflict of $P_{con,AB} = 100\%$. The costs related to each aircraft (see Equation (18)) are $J_A = J_B = 0.5$. After the CR, by modifying the aircraft trajectories, the conflict probability drops below the probability threshold to $P_{con,AB} = 45\%$. The horizontal profile of the trajectories of the two aircraft is represented in Figure 5(b); the nominal trajectories are depicted with dotted lines, and the resolution trajectories are shown with solid lines. For this particular conflict situation, one of the waypoints of the trajectory of aircraft B is modified to allow the safe separation between the aircraft around the crossing point, while aircraft A maintains its original trajectory. The cost associated to each trajectory after the conflict resolution is $J_A = 0$ and $J_B = 1.577 \cdot 10^{-2}$. As a consequence of the resolution maneuver, aircraft B flies an additional distance of 2.937 km.

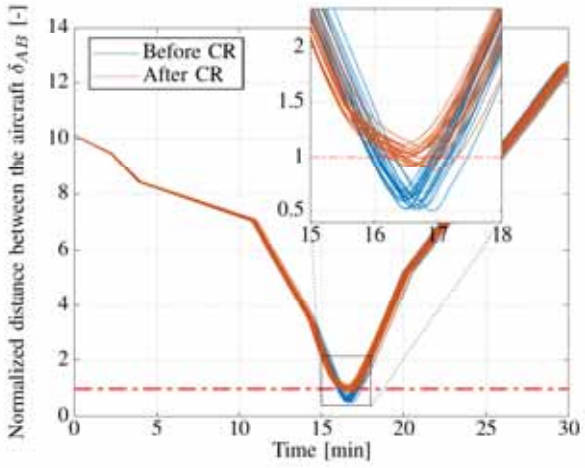

(a) Normalized distance between the aircraft.

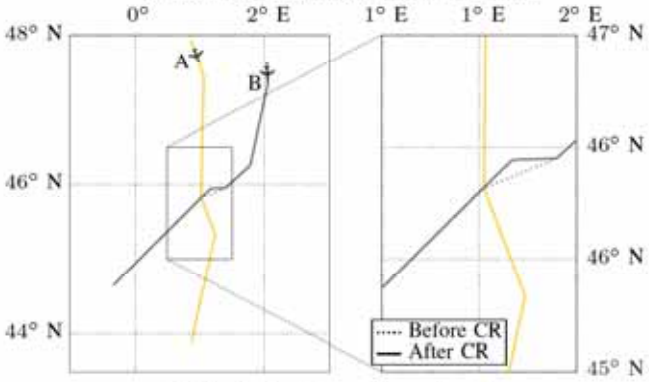

(b) Nominal and resolution trajectories.

Figure 5. Example of the effects of the CR method on the aircraft trajectories.

The effects of the CD&R methodology on the whole conflict scenario with $N = 822$ aircraft is presented next. The results of the conflict detection process before the conflict resolution, along with the nominal paths of the aircraft, are depicted in Figure 6(a) and Figure 6(b) for the horizontal and vertical profiles, respectively. In total, 185 conflicts are detected: 29 of these conflicts are low-probability conflicts (with a probability of conflict below the probability threshold $P_{con,ij} \leq 50\%$; the locations of the aircraft at the point of closest approach are represented with blue marks); 131 of them are high-probability conflicts ($P_{con,ij} \geq 50\%$, represented with red marks); and 25 are tactical conflicts (the aircraft are in loss of separation at the starting time, $\eta_{ij} = 1$, represented by orange marks). The nominal value of the cost function is $J_0 = 124.35$.

The resolution trajectories, obtained after the application of the CR methodology, are depicted in Figures 6(c) and 6(d); both the horizontal and vertical profiles are represented, as well as the locations of the detected conflicts. A visual representation of the effects of the CR process on the number of conflicts is presented in Figure 7. The total number of conflicts detected after the CR process is 146. There is a significant drop in the number of high-probability conflicts, which decreases from 131 to only 14. The remaining 14 unsolved conflicts correspond to encounters that are too severe to be solved within the constraints described in Section IV-B. The number of low-probability conflicts increases from 29 to 107, which illustrates that some of the high-probability conflicts present before the CR process lower their conflict probability below 50%, whereas for some of them the conflict probability directly drops to zero. The number of tactical conflicts remains the same; these conflicts are not the target of the proposed methodology, and should be solved tactically. The value of the cost function is reduced to $J_{best} = 17.204$. These results are summarized in Table I. Some indicators of the cost of the conflict resolution on the aircraft trajectories are also collected in this Table. The total number of aircraft that modified their trajectories in the conflict resolution is 160. The lateral deviation parameter $A_i/L_{0,i}$ of these modified trajectories presents an average value of 0.20 m and a maximum of 2.71 m. As a consequence of the resolution maneuvers, the modified trajectories differ in length by an average of 3.89 km and a maximum of 20.52 km from the nominal ones. In most cases, this difference in length comes from the aircraft flying an additional distance (123 aircraft of the total of 160 that modified their trajectories experiment an increase in their flown distance, with an average of 4.62 km additional flight length); on the other hand, a smaller number of aircraft experiment a decrease on the total flown distance (37 aircraft fly shorter paths, with an average of 1.45 km length reduction).

TABLE I. CD&R RESULTS SUMMARY.

		Nominal scenario	After CR
Cost function J		124.35	17.204
Number of conflicts	High-probability	131	14
	Low-probability	29	107
	Tactical	25	25
	Total	185	146
Number of modified trajectories		-	160
Lateral deviation $A_i/L_{0,i}$	Average	-	0.20 m
	Maximum	-	2.71 m
Flight length difference	Average	-	3.89 km
	Maximum	-	20.52 km

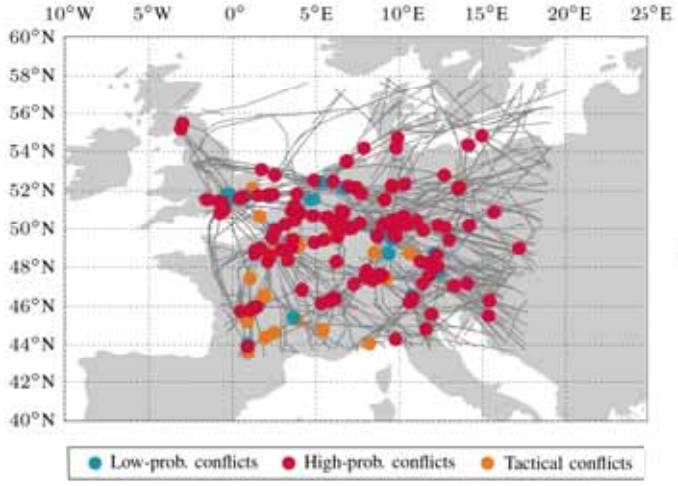

(a) Before CR. Horizontal profiles.

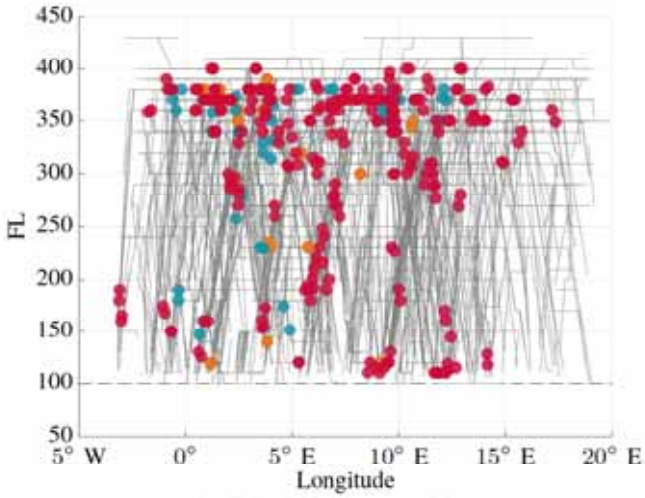

(b) Before CR. Vertical profiles.

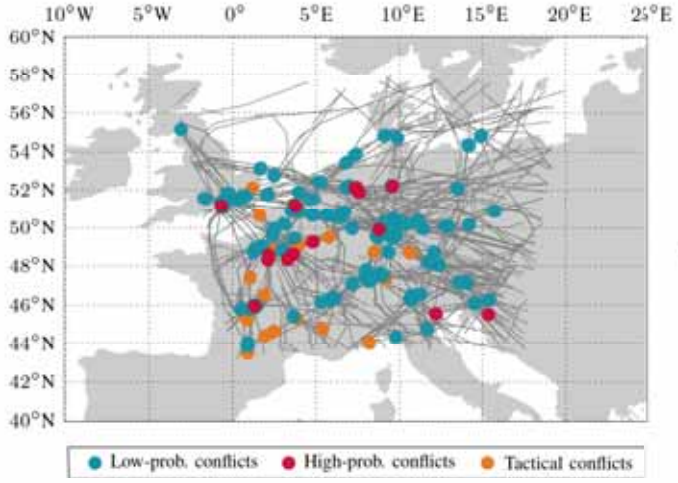

(c) After CR. Horizontal profiles.

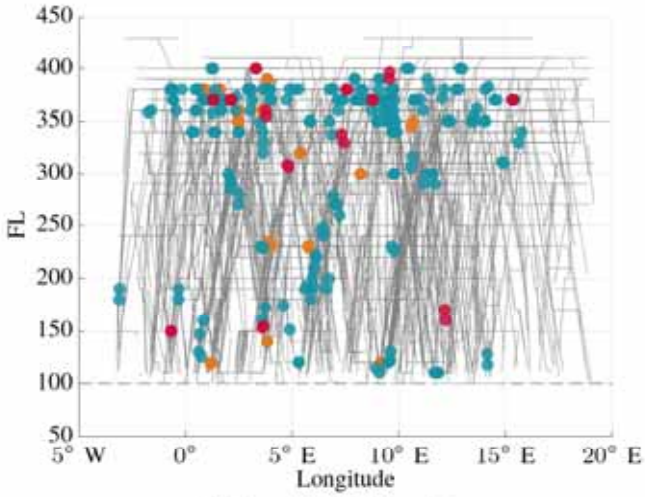

(d) After CR. Vertical profiles.

Figure 6. Aircraft trajectories and conflicts' locations: before, (a) and (b), and after the conflict resolution, (c) and (d).

The predicted losses of separation occur at all stages of the flight, between aircraft that maintain level flight and ascending or descending aircraft. The number of conflicts detected for different flight stages are collected in Table II, before and after the conflict resolution. As these results show, most conflicts take place between level-flight aircraft (47.03% in the nominal scenario and 55.45% in the resolution scenario). The second most common type of conflict would occur between level-flight and descending aircraft, with 22.7% of the cases before CR, and 20.55% after. The less frequent type of conflict would be between ascending and descending aircraft (6% in the nominal scenario and 3% after CR); however, it is important to notice that the conflict methodology is applied in this analysis only to flight levels above 10000 ft, and conflicts between ascending and descending aircraft could be more common at lower altitudes. It can also be observed that the discussed percentages are not significantly affected by the resolution process.

VII. Conclusions

In this paper, a probabilistic methodology for strategic conflict detection and resolution, up to 60 minutes in advance, under wind and temperature uncertainties has been described. The proposed methodology allows the computation of the probability of conflict for pairs of aircraft flying three-dimensional trajectories in a conflict scenario with hundreds of aircraft. Given the aircraft flight plans and the probabilistic

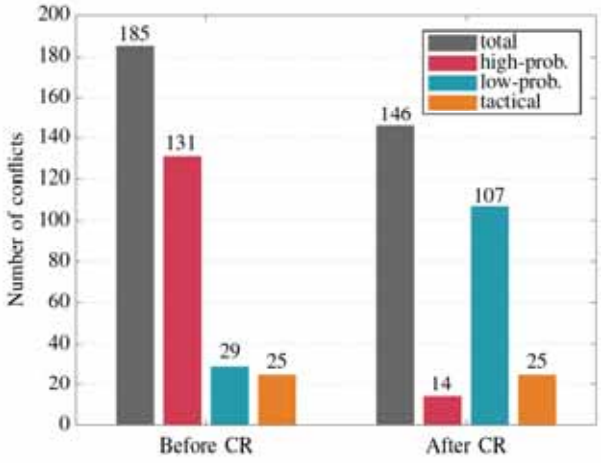

Figure 7. Number of conflicts before and after the conflict resolution.

TABLE II. CONFLICT DETECTION IN DIFFERENT FLIGHT STAGES.

	Nominal scenario		After CR	
Level-level	87	(47.03%)	81	(55.45%)
Level-descent	42	(22.7%)	30	(20.55%)
Level-climb	29	(15.68%)	19	(13.01%)
Descent-descent	14	(7.57%)	10	(6.85 %)
Climb-climb	7	(3.78%)	3	(2.05%)
Climb-descent	6	(3.24%)	3	(2.05%)
Total	185	(100%)	146	(100%)

weather forecast provided by the EPS, the proposed grid-based CD method is able to efficiently compute the probability of conflict between hundreds of aircraft. The conflicts between the aircraft are classified in high-probability, low-probability, and tactical conflicts. The conflict resolution methodology is capable of generating resolution trajectories that significantly lower the number of high-probability conflicts.

The methodology has been successfully applied to a realistic case study; in particular, actual flight plans for aircraft flying in an European area over a time interval of 60 minutes are considered. The numerical results show that the number of high-probability conflicts can be significantly reduced. The proposed methodologies aim to expand the capabilities of conflict detection and resolution tools currently in use in Europe, enabling the planning of more efficient trajectories and reducing the workload of air traffic controllers.

Future steps in this line of research involve the expansion of the methodologies to consider departing and arriving flights below flight level FL100 and an extended geographical area. The development of this expanded methodology will require the consideration of additional sources of uncertainty, such as the aircraft departure times, and will also involve the integration of different global and regional Ensemble Prediction Systems to widen the coverage area. An interesting approach that would improve the scalability of the methodology is the integration of clustering techniques that would allow the subdivision of the global CR problem into distinct smaller and parallelizable subproblems. Another future work is the consideration of other types of resolution strategies, such as speed or altitude changes.

ACKNOWLEDGMENT

The authors gratefully acknowledge the financial support of the Spanish Ministerio de Ciencia, Innovación y Universidades through Grant RTI2018-098471-B-C31.

REFERENCES

[1] D. Rivas and R. Vazquez, "Uncertainty," in Complexity Science in Air Traffic Management, A. Cook and D. Rivas Ed., Ashgate Publishing Limited, 2016, Chap. 4.

[2] World Meteorological Organization, "Guidelines on Ensemble Prediction Systems and Forecasting," WMO-No. 1091, 2012.

[3] A. Franco, D. Rivas, and A. Valenzuela, "Probabilistic aircraft trajectory prediction in cruise flight considering ensemble wind forecasts," *Aerospace Science and Technology*, Vol. 82–83, 2018, pp. 350–362.

[4] E. Hernández-Romero, A. Valenzuela, and D. Rivas, "A probabilistic approach to measure aircraft conflict severity considering wind forecast uncertainty," *Aerospace Science and Technology*, Vol. 86, 2019, pp. 401–414.

[5] E. Hernández-Romero, A. Valenzuela, and D. Rivas, "Probabilistic Multi-Aircraft Conflict Detection and Resolution considering Wind Forecast Uncertainty," *Aerospace Science and Technology*, Vol. 105, 2020.

[6] D. Delahaye, C. Peyronne, M. Mongeau, and S. Puechmorel, "Aircraft Conflict Resolution by Genetic Algorithm and B-Spline Approximation," in *EIWAC 2010, 2nd ENRI International Workshop on ATM/CNS*, 2010, pp. 71–78.

[7] Allignol C., Barnier N., Durand N., Gondran A., and Wang R., "Large Scale 3D En-Route Conflict Resolution," in *Proc. 12th Traffic Management Research and Development Seminar (ATM2017)*, 2017, pp. 1–8.

[8] O. Rodionova, B. Sridhar, and H. K. Ng, "Conflict resolution for wind-optimal aircraft trajectories in North Atlantic oceanic airspace with wind uncertainties," in *Proceedings on the 2016 IEEE/AIAA 35th Digital Avionics Systems Conference (DASC)*, 2016, pp. 1–10.

[9] S. Chaimatanan"Planification stratégique de trajectoires d'avions," PhD Thesis. Université Toulouse III-Paul Sabatier, 2014.

[10] V. Courchelle, M. Soler, D. Gonzlez-Arribas, and D. Delahaye, "A simulated annealing approach to 3D strategic aircraft deconfliction based on en-route speed changes under wind and temperature uncertainties," *Transportation Research Part C: Emerging Technologies*, Vol. 103, 2019, pp. 194–210.

[11] E. Hernández-Romero, A. Valenzuela, D. Rivas and D. Delahaye, "Metaheuristic Approach to Probabilistic Aircraft Conflict Detection and Resolution Considering Ensemble Prediction Systems," in *Proc. 9th SESAR Innovation Days (SID)*, pp. 1–8, 2019.

[12] M. Jardin, "Grid-based strategic air traffic conflict detection," *AIAA Guidance, Navigation, and Control Conference and Exhibit*, San Francisco, California, 2005, pp. 1–11.

[13] S. Kirkpatrick, C. D. Gelatt, and M. P. Vecchi, "Optimization by simulated annealing," *Science*, Vol. 220, No. 4598, 1983, pp. 671–680.

[14] M. Baldauf, C. Gebhardt, S. Theis, B. Ritter, and C. Schraff, "Beschreibung des operationellen Kürzestfristvorhersagemodells COSMO-D2 und COSMO-D2-EPS und seiner Ausgabe in die Datenbanken des DWD," Deutscher Wetterdienst (DWD), Offenbach, Germany, 2018.

[15] Deutscher Wetterdienst, "NWP forecast data," https://www.dwd.de/EN/ourservices/nwp_forecast_data/nwp_forecast_data.html, accessed: 2019-04.

[16] A. Nuic, "User Manual for the Base of Aircraft Data (BADA) Revision 3.13," EEC Technical/Scientific Report No. 15/04/02-43, EUROCONTROL Experimental Centre, 2015.